Temperature effects on the modal properties of a suspension bridge

Etienne Cheynet[1,*], Jonas Snæbjörnsson[1,2] and Jasna Bogunović Jakobsen[1]

[1]Department of Mechanical and Structural Engineering and Materials Science, University of Stavanger, N-4036 Stavanger, Norway

[2]School of Science and Engineering, Reykjavik University, Menntavegur 1, 101 Reykjavík, Iceland

Corresponding author: Etienne Cheynet, etienne.cheynet@uis.no

Abstract

The paper studies temperature effects on the modal parameters of a suspension bridge across a Norwegian fjord. The approach used is a full-scale ambient vibration testing, where an automated Covariance-Driven Stochastic Subspace Identification (SSI-COV) method is used to identify the modal parameters. The bridge site, the bridge structure and the monitoring system are presented, followed by a summary of the data analysis procedure and the parameters used for the automated SSI-COV method applied. The operational modal analysis is based on 6 months of continuous acceleration records providing seasonal and diurnal variations of the natural frequencies of the bridge and the modal damping ratios. Temperature effects were observed with details that are scarcely available in the literature. In particular, the daily fluctuations of natural frequencies and seasonal effects were more pronounced than expected. The influence of other environmental effects that may affect the estimated parameters are discussed.

Keywords Suspension bridge; Full-scale; Ambient vibrations; Modal parameters; Temperature effects.

1 Introduction

Ambient Vibration Testing (AVT) has become the "default procedure" for modal parameter identification of cable-supported bridges [4]. AVT is particularly attractive for studying environmental effects on the modal parameters, such as the evolution of the modal damping ratios of suspension bridge with increased mean wind velocity [3, 5, 9, 13]. Other environmental effects, such as daily and seasonal fluctuations of temperature, are also known to influence the eigen-frequencies of concrete bridges [11, 14] and suspension bridges [6, 8]. During the last few years, several studies have focused on modelling the thermal behaviour of the entire bridge structure [2, 18, 22] and on measuring the static displacements induced by thermal loading [19, 21]. On the other hand, relatively few studies have been dedicated to the investigation of temperature effects on the modal properties of a suspension bridges using AVT, based on large amount of ambient vibration data.

The present paper illustrates the influence of daily temperature fluctuations on the eigen frequencies and modal damping ratios of the Lysefjord bridge, which is located at the inlet of a fjord in Norway. The automated Covariance-Driven Stochastic Subspace Identification (SSI-COV) algorithm developed by Magalhães et al. [11] has been used to identify the modal parameters of the bridge. This algorithm was applied by e.g. Magalhães and Cunha [10] on an arch bridge using more than 2 years of data and by Brownjohn et al. [4] on a long-span suspension bridge using only a couple of days of data. The present study therefore complements the study of Magalhães and Cunha [10] and Brownjohn et al. [4] by utilising 6 months of continuous vibration measurements conducted on a long-span suspension bridge.

The present paper is organised as follows: first, the bridge site and instrumentation are presented, followed by a short summary of the parameters used with the automated SSI-COV algorithm. Then the influence of the daily temperature fluctuations on the bridge eigen-frequencies is demonstrated and discussed. Finally, the evolution of the modal damping ratios with temperature variations are investigated.

2 Instrumentation and methods

2.1 The bridge site

The Lysefjord Bridge, positioned at the narrow inlet of a fjord in the South-West part of the Norwegian coast, is used as a case study. Its main span is 446 m, with the central part 55 m above the sea level. The bridge is entrenched between two

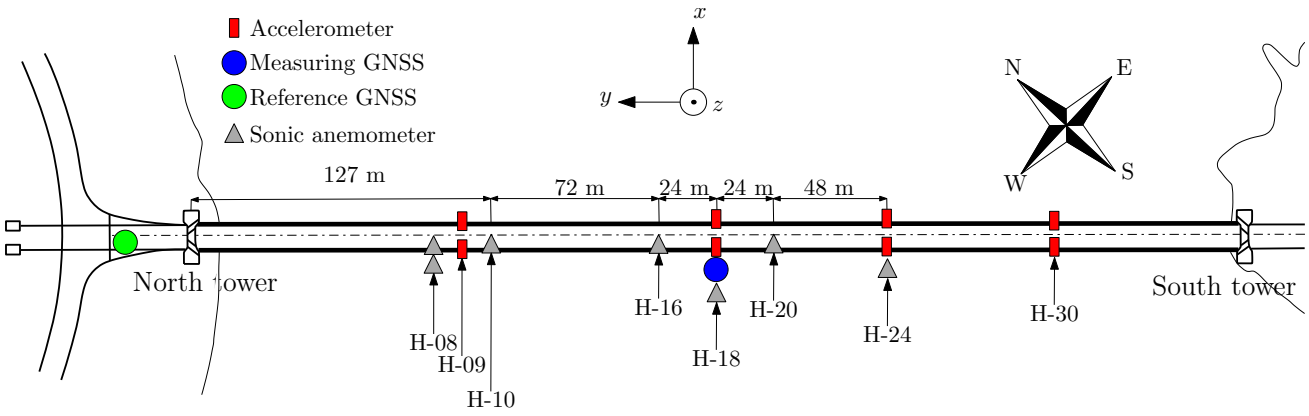

Figure 1. Wind and Structural Health Monitoring System installed on the Lysefjord Bridge.

steep hills with slopes ranging from 30° to 45° and a maximum altitude of 350 m to the North and 600 m to the South. The bridge is exposed to winds that may descent from mountains nearby or follow the fjord over a longer path. The West side of the bridge is exposed to a more open and levelled area.

Since 2013, the bridge has been instrumented with 7 sonic anemometers installed on the West side of the bridge deck and four pairs of accelerometers located inside the deck (Fig. 1). GPS timing is used to synchronize the wind- and acceleration data, acquired locally with separate data logging units. Although the highest sampling frequency of the accelerometers and anemometers is 200 Hz and 32 Hz respectively, the data are acquired with a sampling frequency of 50 Hz and decimated to 20 Hz to facilitate data handling. Finally, a 3G router enables wireless data access and transfer via a mobile network. A more detailed description of the bridge instrumentation is given in e.g. [5]. Temperature measurements are provided by a Vaisala weather transmitter WXT520 located on hanger 10, denoted H-10, whereas the accelerometers are located near hangers 9, 18, 24 and 30, where hanger 18 corresponds to the mid-span position.

2.2 *Automated SSI-COV procedure*

The automated SSI-COV method developed by Magalhães et al. [11] is applied on 6 months of acceleration records obtained from July 2015 to December 2015. For the sake of brevity, the automated SSI-COV method used will not be described explicitly in this paper but the details can be found in e.g. [10, 11]. The parameters used to calibrate this automated SSI-COV method are summarized in Table 1.The minimal and maximal order of the system for the calculation of the stabilization diagram are denoted $N_{\min}$ and $N_{\max}$ respectively, whereas $\tau_{\max}$ is the maximal time lag used to compute the cross-covariance matrix. The three accuracy thresholds for the identified eigen-frequencies, modal damping ratios and modal assurance criterion [1] are denoted ε_{fn}, ε_{ζ} and ε_{MAC} respectively. Finally, the threshold accuracy for the cluster analysis is ε_{d}.

The mode shapes and eigen-frequencies of the Lysefjord Bridge were successfully identified by the automated SSI-COV method used in the present study [5]. The modal parameters are hereby denoted using the code XYZ, where X = {H, V, T} represents the lateral (H), vertical (V) and torsional (T) bridge motion. Y = {S, A} is the symmetric (S) or asymmetric (A) mode shape, and Z the mode number. For example HS1 refers to the first symmetric horizontal mode shape, and TA2 refers to the second asymmetric torsional mode shape. To increase the identification speed of the lower modes, the sampling frequency of the lateral and vertical acceleration records were reduced to 2 Hz. The sampling frequency of the torsional acceleration response remained at 20 Hz. This allowed the SSI-COV algorithm to be applied to more than 50 000 acceleration records of 10 min duration in less than half a day.

A Finite element (FE) model created with the software Abaqus by Steigen [15] and improved by Tveiten [17] was used to evaluate a numerical prediction of the mode shapes and eigen-frequencies of the Lysefjord Bridge. The eigen-frequencies and the mode shapes of the Lysefjord Bridge were also approximated by using harmonic series expansions following Sigbjörnsson and Hjorth-Hansen [12] for the lateral motion and Strømmen [16] for the vertical and torsional ones. In the following, the latter method is referred to as the "Simplified Bridge Model" denoted SBM.

Table 1. Parameters used in the SSI-COV method applied on Lysefjord bridge acceleration data.

$\tau_{\max}$ (s)	$N_{\min}$	$N_{\max}$	ε_{fn}	ε_{ζ}	ε_{MAC}	ε_{d}
15	3	30	5e − 3	3e − 2	5e − 3	2e − 2

Table 2. Eigen-frequencies calculated using the SSI-COV method with the values calculated using the Abaqus model and the SBM.

Modes	SSI-COV	SBM		Abaqus	
	Hz	Hz	%	Hz	%
HS1	0.136	0.130	-4.41	0.128	-6.19
HA1	0.444	0.442	-0.45	0.431	-2.90
HS2	0.577	0.556	-3.51	0.533	-7.56
HA2	0.626	0.597	-4.61	0.583	-6.81
HS3	0.742	0.830	11.90	0.833	12.31
HA3	1.011	1.000	-1.03	0.974	-3.69
VA1	0.223	0.205	-8.10	0.214	-3.91
VS1	0.294	0.319	8.35	0.302	2.72
VS2	0.408	0.439	7.63	0.407	-0.25
VA2	0.587	0.585	-0.39	0.583	-0.68
VS3	0.853	0.864	1.31	0.856	0.34
VA3	1.163	1.194	2.72	1.191	2.36
TS1	1.237	1.215	-1.78	1.238	0.026
TA1	2.184	2.186	0.09	2.122	-2.85

3 Results

3.1 Influence of temperature variations on the eigen-frequencies

As stated by Xia et al. [20], a higher temperature leads in general to decreased values of vibration frequencies, mainly due to the temperature dependency of the materials Young's modulus. This variation of the eigen-frequencies are visible in Fig. 2, except for temperatures over 20 °C where the amount of samples was probably too low to provide reliable results. The influence of temperature variations on the first lateral mode HS1 is rather small. The frequency drops from 0.139 Hz to 0.135 Hz when the temperature increases from 0 °C to 20 °C. For a similar temperature change, the frequency associated with VA1 decreases only from 0.227 Hz to 0.220 Hz. The most dramatic frequency change occurs for the mode TS1 where the frequency decreases from 1.25 Hz to 1.23 Hz. The scatter of the eigen-frequencies observed on Fig. 2 is due to the influence of other parameters such as traffic, the mean wind velocity and maybe wind turbulence. The daily fluctuations of the eigen-frequencies can be visualized by studying few days of data. This is done in Fig. 3, where ten days of data recorded in October 2015 are displayed. The first lateral eigen-frequency HS1 fluctuates between 0.132 Hz for diurnal data and 0.145 Hz for nocturnal data. These fluctuations are relatively small compared to those from VA1 which ranges from 0.217 Hz at day time to almost 0.230 Hz during the night. For the torsional motion, TS1 fluctuates between 1.25 Hz down to 1.23 Hz.

As suggested by Kim et al. [7], heavy traffic is likely to be responsible for a decrease in the estimated eigen-frequencies of the bridge deck. The effects of the temperature and traffic on the bridge eigen-frequencies are therefore expected to superimpose and be responsible for larger frequency variations. At night time, the lower temperature and the reduced traffic leads to higher eigen-frequencies whereas at day time, the increase of the temperature and traffic leads to lower eigen-frequencies. This appears clearly on Fig. 3, where a pseudo-period of 24 h is visible. The periodical pattern is clearly visible for the vertical bridge motion, but it is more noisy for the lateral and torsional motions. This can be partly explained by the higher signal to noise ratio measured for the vertical motion.

Temperature fluctuations seem to have a larger influence on the variation of the eigen-frequencies than the traffic loading. The attenuation of the daily periodicity of the eigen-frequency in November and December (Fig. 4) cannot simply be explained by a reduction of heavy traffic for example. The periodicity pattern appears to be almost entirely modulated by temperature changes. For example, we observed that the sinusoidal pattern was flatter on its bottom in July (longer day) and flatter on its top in October (shorter day), without strong variations in the amplitude of the fluctuations.

3.2 Influence of temperature variations on the modal damping ratios

The estimation of the modal damping ratios is one of the most crucial step in studying accurately the buffeting response of a suspension bridge. Unfortunately, such studies are a rarity in full scale. In general, the aerodynamic damping ratios are obtained with a large dispersion in full-scale [3, 13]. This requires a statistically significant amount of data, which is rarely observed in the literature. In this subsection, the total damping is considered for various wind conditions, using a considerable amount of data. The evolution of the modal damping ratios with the mean wind velocity has been described in e.g. Cheynet et al. [5] and is therefore not recalled here.

Temperature effects on the modal damping ratios remain mostly unexplored and are therefore briefly investigated in the following. The variation of the modal damping ratios with temperature is displayed in Fig. 5, for the first four lateral and

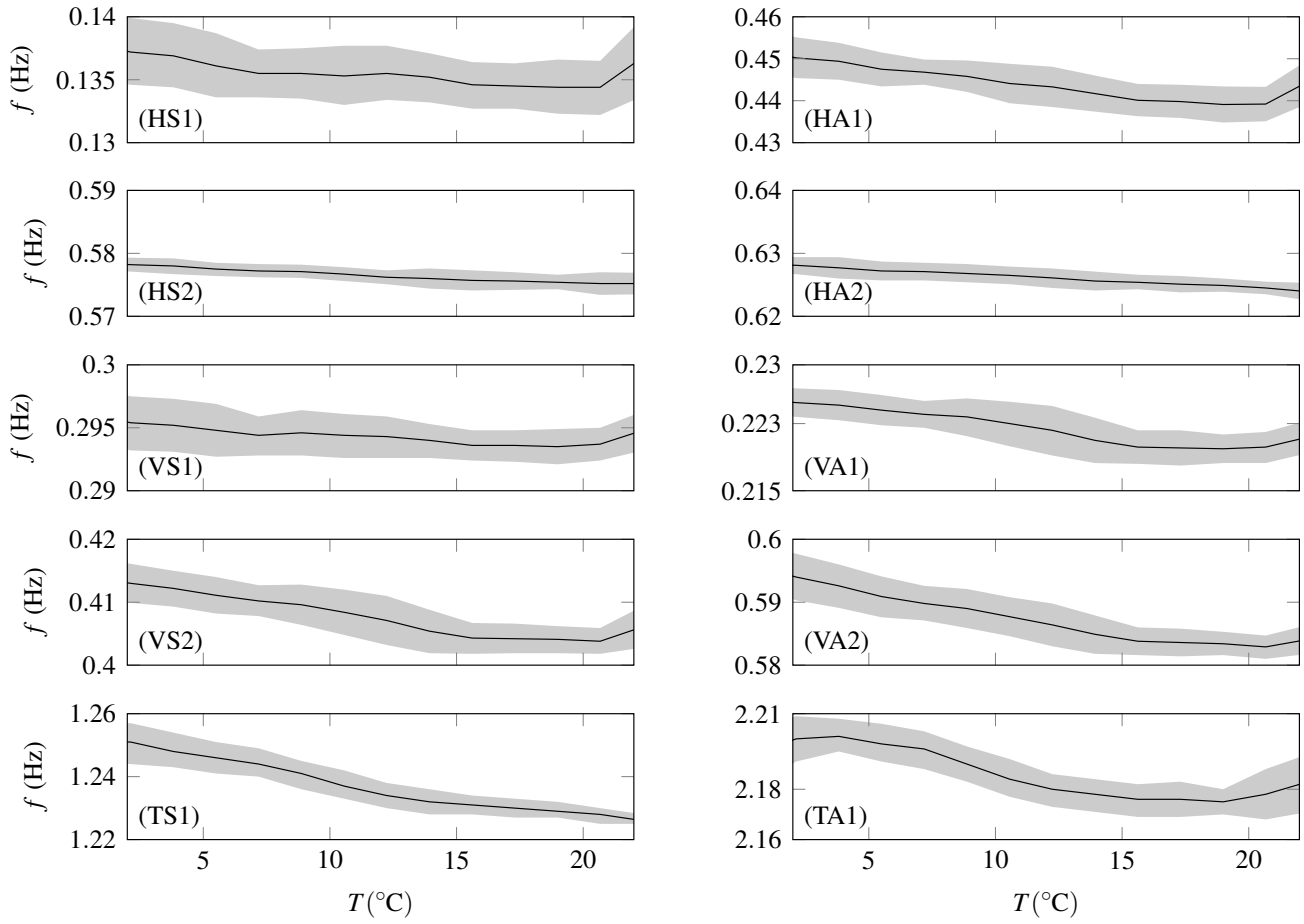

Figure 2. Evolution of the first four lateral and vertical and the first two torsional eigen-frequencies with the temperature. The data set comprises six months of acceleration and temperature records (July to December 2015).

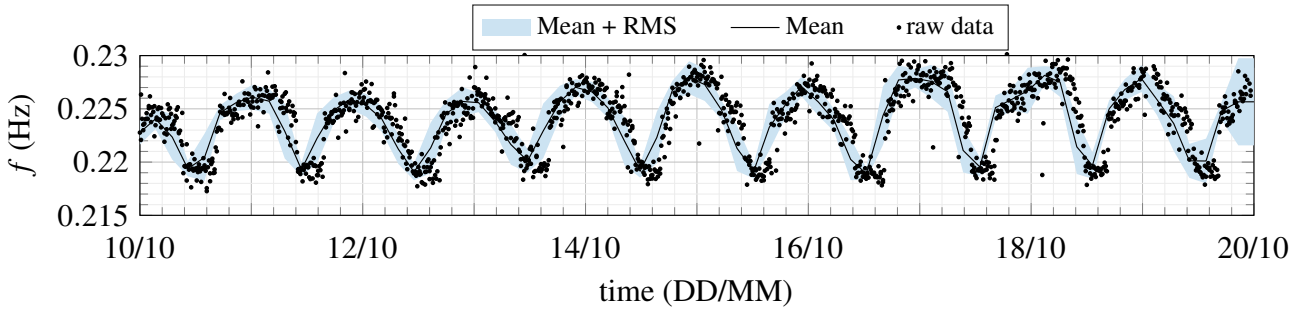

Figure 3. Evolution of HS1 (top), VA1 (middle) and TS1 (bottom) between the 20/09/2015 and 30/09/2015. Data binning has been applied to better estimate the fluctuating mean value and RMS of the eigen-frequencies.

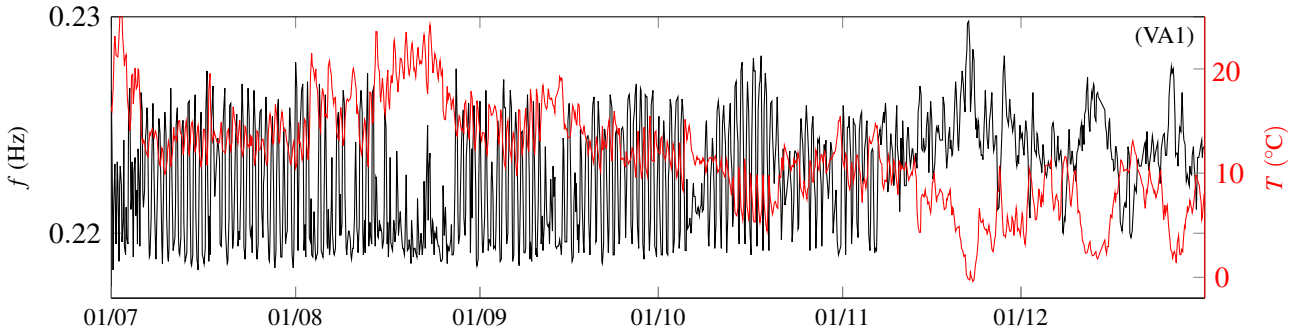

Figure 4. Evolution of the temperature and the frequency of the mode VA1 from July 2015 to December 2015.

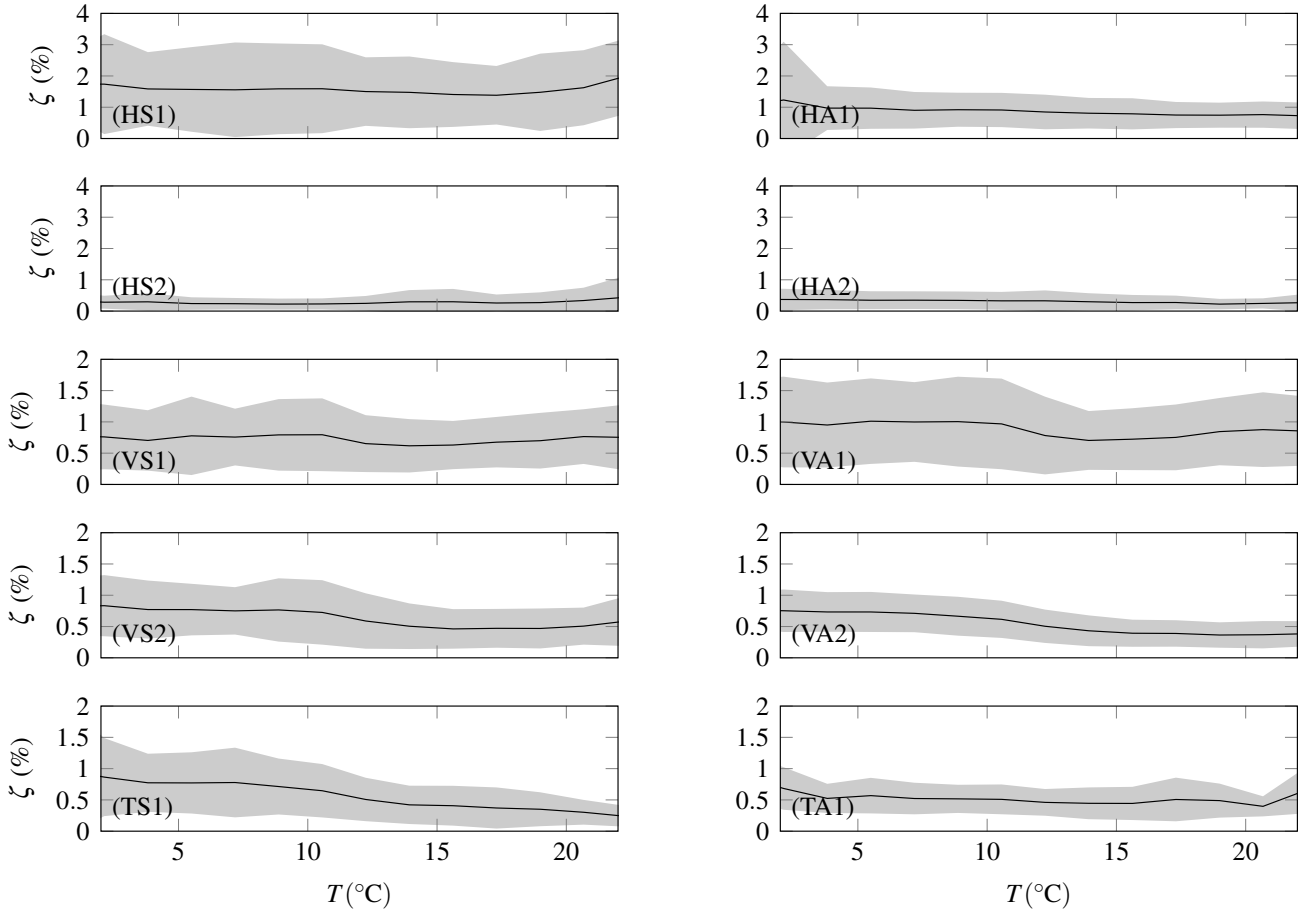

Figure 5. Modal damping ratios expressed as a function of the temperature for the first four lateral and vertical modes and the first two torsional modes, based on acceleration data recorded from July 2015 to December 2015.

vertical modes as well as the first two torsional modes.

As expected, the damping ratios for HS1, HS2, HA2, VS1, VA1 and TA1 fluctuate little with the temperature. For a given temperature, multiple wind velocities are recorded. Because the total modal damping ratios increase with the wind velocity, due to added aerodynamic damping, a large variety of total modal damping ratios are recorded for a given temperature. Consequently, a large dispersion is expected when the modal damping ratios are expressed as a function of the temperature alone. On Fig. 5, VS1 and VA1 have an averaged modal damping ratios of about 0.75% and 1% respectively and are characterized by a considerable spreading. This is not surprising given that the modal damping ratios associated with VS1 and VA1 are highly affected by the wind induced aerodynamic damping effect [5].

A reduction in modal damping with increasing temperatures and the underlying reduction in wind speed is expected for other modes. This is in particular the case for the vertical modes for which the aerodynamic damping can be relatively high. Highest damping values are still observed for temperatures between 5 °C and 10 °C at which the strongest winds occur.

A decrease of the damping ratios of TS1 for increasing temperatures is somewhat more distinct. As already pointed out,

lower temperatures are typically associated with higher wind speeds, for which a weakly increasing TS1 damping ratio has been observed [5]. It is however a bit surprising that the corresponding contribution of the aerodynamic damping, which is much stronger for the vertical modes, is not so obvious in the average damping estimates presented. To improve the reliability of these results, an analysis using at least one year of temperature, velocity and acceleration data is required.

4 Conclusions

The modal parameters of the Lysefjord bridge have been identified using AVT based on an automated SSI-COV procedure relying on several months of continuous acceleration records. Environmental effects were observed with a level of details that is scarcely available in the literature. In particular, the daily fluctuations of the eigen-frequencies were remarkably well captured as was the possible temperature-dependency of the modal damping ratios. A relatively large amount of acceleration data was accumulated, so that a statistical description of the influence of the mean wind velocity on the modal damping ratios could be achieved. Application of OMA using the automated SSI-COV method on other suspension bridges in complex terrain may provide a better general understanding of environmental influence on the modal parameters of long-span suspension bridges.

The good agreement between the computed natural frequencies and the measured ones is encouraging to proceed further with the investigation of full-scale measurement data using the automated SSI-COV method. The modal analysis also documented the non-linearity of the modal damping ratios and a possible non-negligible role of temperature effects on the modal parameters of the bridge. Further analysis will consider at least one year of full-scale measurements, and a more severe segregation of wind samples characterized by unusually high turbulence intensity indicating non-stationary fluctuations in excitation and response.

References

[1] Randall J Allemang and David L Brown. A correlation coefficient for modal vector analysis. *Proceedings of the 1st international modal analysis conference*. Vol. 1. SEM, Orlando. 1982, pp. 110–116.

[2] Nicholas de Battista, James M.W. Brownjohn, Hwee Pink Tan, and Ki-Young Koo. Measuring and modelling the thermal performance of the Tamar Suspension Bridge using a wireless sensor network. *Structure and Infrastructure Engineering* **11**.2 (2015), pp. 176–193. DOI: *10.1080/15732479.2013.862727*.

[3] JMW Brownjohn, AA Dumanoglu, RT Severn, and CA Taylor. Ambient vibration measurements of the Humber suspension bridge and comparison with calculated characteristics. *Proceedings of the Institution of Civil Engineers* **83**.3 (1987), pp. 561–600.

[4] JMW Brownjohn, Filipe Magalhaes, Elsa Caetano, and Alvaro Cunha. Ambient vibration re-testing and operational modal analysis of the Humber Bridge. *Engineering Structures* **32**.8 (2010), pp. 2003–2018. DOI: *10.1016/j.engstruct.2010.02.034*.

[5] Etienne Cheynet, Jasna Bogunović Jakobsen, and Jónas Snæbjörnsson. Buffeting response of a suspension bridge in complex terrain. *Engineering Structures* **128** (2016), pp. 474–487. DOI: *10.1016/j.engstruct.2016.09.060*.

[6] YouLiang Ding and AiQun Li. Temperature-induced variations of measured modal frequencies of steel box girder for a long-span suspension bridge. *International Journal of Steel Structures* **11**.2 (2011), pp. 145–155. DOI: *10.1007/s13296-011-2004-4*.

[7] Chul-Young Kim, Dae-Sung Jung, Nam-Sik Kim, Soon-Duck Kwon, and Maria Q Feng. Effect of vehicle weight on natural frequencies of bridges measured from traffic-induced vibration. *Earthquake Engineering and Engineering Vibration* **2**.1 (2003), pp. 109–115. DOI: *10.1007/BF02857543*.

[8] KY Koo, JMW Brownjohn, DI List, and R Cole. Structural health monitoring of the Tamar suspension bridge. *Structural Control and Health Monitoring* **20**.4 (2013), pp. 609–625.

[9] John H.G. Macdonald. Evaluation of buffeting predictions of a cable-stayed bridge from full-scale measurements. *Journal of Wind Engineering and Industrial Aerodynamics* **91**.12âĂŞ15 (2003), pp. 1465 –1483. ISSN: 0167-6105. DOI: *10.1016/j.jweia.2003.09.009*.

[10] Filipe Magalhães and Àlvaro Cunha. Explaining operational modal analysis with data from an arch bridge. *Mechanical Systems and Signal Processing* **25**.5 (2011), pp. 1431 –1450. ISSN: 0888-3270. DOI: *10.1016/j.ymssp.2010.08.001*.

[11] Filipe Magalhães, Àlvaro Cunha, and Elsa Caetano. Online automatic identification of the modal parameters of a long span arch bridge. *Mechanical Systems and Signal Processing* **23**.2 (2009), pp. 316 –329. ISSN: 0888-3270. DOI: *10.1016/j.ymssp.2008.05.003*.

[12] Ragnar Sigbjörnsson and Erik Hjorth-Hansen. Along-wind response of suspension bridges with special reference to stiffening by horizontal cables. *Engineering Structures* **3**.1 (1981), pp. 27–37.

[13] Dionysius M Siringoringo and Yozo Fujino. System identification of suspension bridge from ambient vibration response. *Engineering Structures* **30**.2 (2008), pp. 462–477. DOI: *10.1016/j.engstruct.2007.03.004*.

[14] Hoon Sohn, Mark Dzwonczyk, Erik G. Straser, Anne S. Kiremidjian, Kincho H. Law, and Teresa Meng. An experimental study of temperature effect on modal parameters of the Alamosa Canyon Bridge. *Earthquake Engineering & Structural Dynamics* **28**.8 (1999), pp. 879–897. ISSN: 1096-9845.

[15] Ragnhild Opsahl Steigen. Modeling and analyzing a suspension bridge in light of deterioration of the main cable wires. MA thesis. University of Stavanger, 2011.

[16] Einar N. Strømmen. Structural Dynamics. Cham: Springer International Publishing, 2014. Chap. Eigenvalue Calculations of Continuous Systems, pp. 89–159. ISBN: 978-3-319-01802-7. DOI: *10.1007/978-3-319-01802-7_3*.

[17] Jan Tveiten. Dynamic analysis of a suspension bridge. MA thesis. University of Stavanger, 2012.

[18] Robert Westgate, Ki-Young Koo, and James Brownjohn. Effect of solar radiation on suspension bridge performance. *Journal of Bridge Engineering* **20**.5 (2014), p. 04014077. DOI: *10.1061/(ASCE)BE.1943-5592.0000668*.

[19] Y Xia, B Chen, XQ Zhou, and YL Xu. Field monitoring and numerical analysis of Tsing Ma Suspension Bridge temperature behavior. *Structural Control and Health Monitoring* **20**.4 (2013), pp. 560–575. DOI: *10.1002/stc.515*.

[20] Y Xia, B Chen, S Weng, YQ Ni, and YL Xu. Temperature effect on vibration properties of civil structures: a literature review and case studies. *Journal of civil structural health monitoring* **2**.1 (2012), pp. 29–46. DOI: *10.1007/s13349-011-0015-7*.

[21] YL Xu, B Chen, CL Ng, KY Wong, and WY Chan. Monitoring temperature effect on a long suspension bridge. *Structural Control and Health Monitoring* **17**.6 (2010), pp. 632–653. DOI: *10.1002/stc.340*.

[22] Linren Zhou, Yong Xia, James MW Brownjohn, and Ki Young Koo. Temperature Analysis of a Long-Span Suspension Bridge Based on Field Monitoring and Numerical Simulation. *Journal of Bridge Engineering* **21**.1 (2016), p. 04015027. DOI: *10.1061/(ASCE)BE.1943-5592.0000786*.